Accepted Manuscript

Please cite this article as: Carretta, Y., Hunter, A.K., Boman, R., Ponthot, J.-P.,
Legrand, N., Laugier, M., Dwyer-Joyce, R.S., Ultrasonic roll bite measurements in
cold rolling – Roll stress and deformation.Journal of Materials Processing Technology
http://dx.doi.org/10.1016/j.jmatprotec.2017.05.036

Ultrasonic roll bite measurements in cold rolling – roll stress and deformation

Y Carretta[1], A K Hunter[2],

R Boman[1], J-P Ponthot[1],

N Legrand[3], M Laugier[3], R S Dwyer-Joyce[2]

[1]Department of Aerospace and Mechanical Engineering, University of Liège, Belgium

y.carretta@ulg.ac.be

r.boman@ulg.ac.be

jp.ponthot@ulg.ac.be

[2] The Leonardo Centre for Tribology, Department of Mechanical Engineering, University of Sheffield,

a.k.hunter@sheffield.ac.uk

r.dwyer-joyce@sheffield.ac.uk

[3]ArcelorMittal Global R&D, Maizières-les-Metz, France

nicolas.legrand@arcelormittal.com

maxime.laugier@arcelormittal.com

Abstract.

In cold rolling of thin metal strip, contact conditions between the work rolls and the strip are of great importance: roll deformations and their effect on strip thickness variation may lead to strip flatness defects and thickness inhomogeneity. To control the process, several online measurements are usually carried out such as the rolling load, forward slip and strip tensions at each stand. Shape defects of the strip are usually evaluated after the last stand of a rolling mill thanks to a flatness measuring roll. However, none of these measurements is made within the roll bite itself due to the harsh conditions taking place in that area.

This paper presents a sensor capable of monitoring roll deformations as well as roll radial stresses in situ and in real time. The sensor emits ultrasonic pulses that reflect from the roll surface. The time-of-flight (ToF) of the pulses is recorded during the testing.

Ultrasonic roll bite measurements in cold rolling – roll stress and deformation

The sensor system was incorporated into a work roll and tested on a pilot rolling mill. Measurements were taken as steel strips were rolled under different strip elongation. Roll deformation and radial stresses obtained from the experimental data are in good agreement with numerical results computed with a cold rolling model developed in non-linear Finite Element software.

Keywords.

Ultrasound, Cold Rolling, Flat Product, Finite element method, Roll Bite, Roll Stress, Roll Deformation.

Nomenclature

z	Acoustic impedance, MRayls
t	Time of Flight (ToF), s
c	Speed of sound, m/s
α	Acoustoelastic constant
R	Reflection coefficient
R_0	Roll radius, mm
d_0	Initial ultrasonic path length (also denoted plug length), mm
δ	Plug length variation, mm
ε	Strain
E	Young's modulus, MPa
ν	Poisson's ratio
$\bar{\varepsilon}^p$	Equivalent plastic strain, -
σ_y	Yield stress, MPa
σ_r	Radial stress, MPa
μ_C	Coulomb's friction coefficient, -
L	Roll bite length, m
T_c, T_s	Strip entry and exit tension, MPa
h_c, h_s	Strip entry and exit thickness, mm
V_R	Velocity of roll, m/min

1. Introduction

This paper presents a numerical validation of a new experimental system that uses ultrasonic sensors to perform measurements in cold rolling, directly at the interface between the work rolls and the strip.

Ultrasonic roll bite measurements in cold rolling – roll stress and deformation

In cold rolling, the interaction between the plastic deformations of the strip and the thermo-elastic deformations of the rolls can lead to flatness defects, which are highly detrimental to further metal processing such as stamping. Montmitonnet (2006), who presented a review of cold strip rolling models, observed that this coupling between the strip and the roll becomes even more important as the strip gets thinner.

To control the process, several measurements are usually carried out on industrial rolling mills. For instance, the rolling load and the forward slip (the relative velocity between the roll and the strip at the exit of the contact zone) are continuously recorded to estimate the friction level within the roll gap. Strip thickness sensors at entry and exit of the stand are used to monitor thickness changes. Also, flatness-measuring rolls are commonly located at the exit of the last stand to assess the quality of the strip.

However, all these measurements are made outside of the roll bite. A better control strategy could be achieved by monitoring phenomena within the contact itself with roll gap sensors. To move towards that goal, Legrand et al. (2014) initiated a European project aiming at measuring friction, heat transfers and lubricant film thickness.

This paper presents the development of an ultrasonic sensor suitable for online measurement in a pilot cold rolling mill. The transducer is based on the reflection of an ultrasonic wave from the interface between the roll and the strip.

Ultrasound has long been used as a non-destructive technique to detect defects within solid bodies. Kräutkramer and Kräutkramer (1975) have reviewed the non-destructive testing techniques for solid material using ultrasonic waves. Increasingly ultrasound has been used to investigate tribological phenomena. This started with Kendall and Tabor (1971) who demonstrated that reflection from a rough surface contact depended on the stiffness of the interface. Baik and Thompson (1984) proposed a quasi-static spring model of reflection; they modelled the rough surface interface as an array of equi-spaced cracks to represent the interface stiffness. Arakawa (1983) performed a series of

3

Ultrasonic roll bite measurements in cold rolling – roll stress and deformation

experiments on different roughness machined surfaces pressed together and showed reflection was also dependent on the wavelength (frequency) of the ultrasound used. Krolikowski and Szczepek (1991) used an elastic rough surface contact model to give a better assessment of interface stiffness and compared this with ultrasonic reflection results, as a method to identify contact parameters. Nagy (1992) used shear polarised ultrasound and showed how this was related to shear stiffness of the interface; proposing that the ratio of shear to normal stiffness could be used to characterise interfaces. Drinkwater et al. (1996) studied the relationship between the ultrasonic reflection and frequency from different roughness interfaces. By showing that the reflection was frequency dependent, whilst measured stiffness was not, they were able to validate the spring model approach. In later experiments, Dwyer-Joyce et al. (2000) used the approach to study various asperity interaction phenomena such as adhesion, plastic deformation, and elastic recovery. Baltazar et al. (2002) created a sophisticated micro-mechanical rough surface contact model (incorporating asperity normal and shear interaction) and compared results with reflection form various rough surface contacts.

Ultrasound has been used to measure continuous thin lubricant layers. Anderson et al. (1999) used ultrasound to detect collapse of the oil film in a mechanical face seal. Dwyer-Joyce et al. (2002) validated models of ultrasonic reflection from thin oil films in hydrodynamic and elasto-hydrodynamic contacts. Hunter et al. (2012) calibrated and validated the ultrasonic reflection method for thin film measurements. These methods have been used to measure oil films in the challenging environment within automotive engines. Takeuchi (2011) installed a sensor in the piston pin and studied the oil film between pin and boss in a motored cylinder block. Smith and Sutton (2011) bonded sensors to a cam shaft journal bearing and measured oil films for various lubricant formulations during fired engine running. Mills et al. (2015) installed sensors in a wet liner and measured the oil film between the liner and the piston rings during fired operation.

4

Ultrasonic roll bite measurements in cold rolling – roll stress and deformation

More recently, Chen et al. (2015) employed ultrasound to monitor the load involved in rolling bearing contacts, by monitoring the tiny change in time of flight as the raceways were compressed; a similar approach is followed in the present work.

This technique is now used for the first time in cold rolling where direct measurements at the roll-strip interface are very challenging. These difficulties stem from the extreme stresses involved (up to 1000 MPa), the small contact length (~5-15 mm) compared to the roll radius (50-500mm), the heat generated by the plastic deformation on the strip on such small distance, the roll speed (up to 500 m/min in the tests), the stand vibrations, etc.

Using ultrasonic sensors, it was possible to measure the roll bite length, the strip thickness variation as well as the roll deflection and stresses. The present paper focuses on roll deformation and stresses measurements. The other type of results is discussed in subsequent publications.

The first two sections of this paper give the theoretical background and present the ultrasonic measurements achieved during the testing of the sensor on a pilot rolling mill operated by ArcelorMittal. Experimental data are then compared to numerical results obtained with METAFOR (2016), an in-house finite element code for the modelling of large strains. The main features of these simulations are described in section 4, and the comparison with experimental measurements is presented in section 5.

2. Background

2.1. Non-destructive measurements using ultrasound

The nature of ultrasound is such that when it reaches an interface between two different media, a proportion of the wave is reflected and some is transmitted (see Figure 1 – a). The amplitude of the reflected signal compared to the initial wave, known as the reflection coefficient R, depends on the acoustic mismatch of the interface materials. Kräutkramer and Kräutkramer (1975) referenced the following well-known equation to quantify the reflection coefficient

5

Ultrasonic roll bite measurements in cold rolling – roll stress and deformation

$$R = \frac{z_2 - z_1}{z_1 + z_2} \tag{1}$$

where z_1 and z_2 are the acoustic impedance (given by the product of the density ρ and the speed of sound c) of the media on either side of the interface.

By using this principle, flaws within materials can be detected through their ultrasonic reflection (see Figure 1 – b). Moreover, their position is obtained from the speed of sound within the media and the time difference between the emitted signal and its reflection t. This distance measurement, known as the time-of-flight (ToF), has been used by engineers for a long time and is well understood.

2.2. Ultrasonic measurements in cold rolling

To achieve measurements during cold rolling, ultrasonic sensors were fitted inside a work roll in order to emit signals towards the outer surface of the roll (see Figure 2).

When an ultrasonic wave strikes a part of the roll surface when out of the roll bite, almost the whole wave is reflected back. This is because the acoustic impedance of air or oil is much lower than that of the solid material. For instance, according to equation (1), the amplitude of the reflected wave at a steel-air interface is 99.98% of the incident wave.

Once the ultrasonic wave reaches the roll bite, a part of the signal is transmitted through the interface while the remaining part is sent back to the transducer. Kendall and Tabor (1971) showed the amount of the signal energy crossing the interface depends on the stiffness of the interface , that is related to the number and distribution of asperity contacts, and the solid and lubricant properties. The stiffness varies non-linearly with contact pressure, from zero (when the surfaces are out of contact) to infinity when complete conformity is achieved.

To sum up, whether or not the sensor is facing the roll bite, a signal is reflected back to the sensor and it is therefore possible to measure a change in time of flight for different positions of the sensors close to the roll bite. This change in time of flight is caused by two effects. The first one is the change in geometry of the roll due to rolling: the distance variation between the sensor position and

6

Ultrasonic roll bite measurements in cold rolling – roll stress and deformation

the roll surface induced by roll deformation (see Figure 3). This distance is denoted "plug length" since the ultrasonic sensors were mounted on a cylindrical plug which was then inserted in a work roll (see section 3 for more details). The second cause is the 'acousto-elastic effect', that is the stress dependence of acoustic wave velocity in elastic media. For instance, Egle and Bray (1976) measured the stress-induced changes in ultrasonic wave speeds for steel used in railroad rails to define a constitutive relationship for an isotropic material.

If a material is subjected to a stress, then the resulting velocity of an acoustic wave passing through the material will change depending on the wave mode as well as the magnitude and orientation of the applied stress.

Chen et al. (2015) have developed equations where they split the effect of deflection and acousto-elasticity when performing ultrasonic measurement, with longitudinal ultrasonic waves, on a raceway in a cylindrical roller bearing. Their goal was to deduce the contact load in the direction of the acoustic waves from the recorded data. Their equations are presented in the paragraphs below and applied to the present configuration to determine the plug length variation and the mean radial stress between the sensors position and the roll surface.

2.2.1. Time of flight change due to roll deflection

The contribution to time of flight change due to geometrical change alone Δt_δ is given by

$$\Delta t_\delta = \frac{2\delta}{(c_{rr})_0} \tag{2}$$

where δ is the plug length variation ($\delta(x) = (d(x) - d_0)$ see Figure 3) and $(c_{rr})_0$ is the unstressed speed of sound of a longitudinal wave in the radial direction.

2.2.2. Time of flight change due to the acousto-elastic effect

The time of flight caused only by the ultrasonic speed change Δt_E (acoustoelastic effect alone) is given by

$$\Delta t_E = \frac{2d_0}{(c_{rr})_0}\left(\frac{-\alpha_{rr}\varepsilon_r}{1 - \alpha_{rr}\varepsilon_r}\right) \tag{3}$$

7

Ultrasonic roll bite measurements in cold rolling – roll stress and deformation

where α_{rr} is the acoustoelastic constant accounting for the change in speed of sound due to stresses, d_0 is the distance between the sensor and the unloaded roll surface and ε_r is the radial strain of the roll due to the applied load.

It is useful to substitute the plug length variation δ in place of the radial strain. Assuming a uni-dimensional stress state, the deflection is given in terms of strain by the following

$$\delta = \varepsilon_r d_0 \tag{4}$$

This gives the change in Time of Flight due to the acousto-elastic effect alone, in terms of the deflection δ, acoustoelastic constant, initial length and unstressed speed of sound.

$$\Delta t_E = \frac{-2d_0\alpha_{rr}\delta}{(c_{rr})_0(d_0 - \alpha_{rr}\delta)} \tag{5}$$

2.2.3. Apparent time of flight change due to phase change

The easiest way to compute the Time of Flight between two ultrasonic signals is to measure the time difference between two characteristic points in the waveform. This technique known as the zero-crossing method is affected by phase shift. Indeed, when a reflection occurs at a contact between two components, both the amplitude and the phase of the signal are affected by contact conditions. Even though, phase change can be useful to determine interfacial properties: Reddyhoff et al. (2005) have used the phase change as an alternative mean to measure oil film thickness. In the present case, phase shift induces a variation of the signal shape that may give inaccurate measurements with ToF.

Consequently, the zero-crossing method is best suited when dealing with ultrasonic reflections from a surface that is not in contact with another component since the boundary does not affect the phase of the reflected signal.

As discussed in section 4, the ToF variation is determined by measuring the distance between the Hilbert envelopes of the ultrasonic signals. Since the Hilbert transform is not affected by phase shift, its effect does not have to be accounted for in the present development.

8

Ultrasonic roll bite measurements in cold rolling – roll stress and deformation

2.2.4. Total change in time of flight and plug length variation

The change in ToF Δt is the sum of the three effects discussed above. Since the effect of phase change does not have to be taken into account here, we obtain the following equation when neglecting the quadratic order of δ

$$\Delta t = \Delta t_\delta + \Delta t_E = \frac{2(1 - \alpha_{rr})d_0\delta}{(c_{rr})_0(d_0 - \alpha_{rr}\delta)} \tag{6}$$

The ToF across the instrumented plug is measured as it rotates across the rolling interface. This is then used to infer the plug length variation δ - knowing the initial plug length d_0 and the material properties (α_{rr} and $(c_{rr})_0$) - by using the following equation

$$\delta = \frac{\Delta t \, (c_{rr})_0 d_0}{2(1 - \alpha_{rr})d_0 + \Delta t \, (c_{rr})_0 \alpha_{rr}} \tag{7}$$

2.2.5. Average radial stress in the plug

The average radial stress σ_r along the ultrasonic path length is estimated by using

$$\sigma_r = E \frac{\delta}{d_0} = E \frac{\Delta t \, (c_{rr})_0}{2(1 - \alpha_{rr})d_0 + \Delta t \, (c_{rr})_0 \alpha_{rr}} \tag{8}$$

where *E* is the roll material's Youngs modulus. This gives a measurement of radial roll stress due to rolling. Note that the radial stresses computed here are due to the roll deformation only; the eventual residual stresses in the roll are neglected.

The roll used during the tests has been machined from stock bar of steel (EN31) which has been annealed to improve machinability. The instrumented plug fitted in the roll is made of the same material. Legrand et al. (2014) provided the details of the chemical composition, which is presented in in Table 1 below. The numerical values of the different parameters involved in the equations above are given in Table 2. The Young's modulus is a typical value for steel which is almost insensitive to alloy elements. The longitudinal speed of sound of the unstressed material $(c_{rr})_0$ and the acoustoelastic constant α_{rr} are determined experimentally during a compression test.

9

Ultrasonic roll bite measurements in cold rolling – roll stress and deformation

3. Apparatus

Experiments were carried out on a pilot rolling mill based at ArcelorMittal's research campus in Maizières-lès-Metz (France). The ultrasonic measurement instrumentation consisted of two piezoelectric transducers, an ultrasonic pulser/receiver (UPR) and a data acquisition system (DAQ). These different components are described in the following paragraphs.

3.1. Ultrasonic sensors

The transducers are simple bond-on longitudinally polarised piezo elements with 10 MHz centre frequency as they provide good penetration into steel and a clear distinct signal.

Original elements, initially disc shaped with a diameter of 7 mm, are modified to form narrow strips (see Figure 4 – a) of 1mm width. In this was the . They are bonded to the transmission material using a strain gauge adhesive that also acts as a couplant (see Figure 4 – b). Piezoelectric elements are then protected with a layer of epoxy (see Figure 4 – c) that also acts to damp the sensor suppressing ringing. The sensing area of the resulting system is approximately the same size as the sensor (i.e. 7mm x 1mm) this means that the spatial resolution is of the order of 1mm in the rolling direction.

The transducers are mounted on a metal plug that is then pressed into a hole drilled within the work roll, such that the generated ultrasonic pulse is reflected from the external surface of the roll. The plug and roll surface are then ground in a single operation. Wires to the transducers are extracted through access holes drilled along the axis of the roll, and connected via a slip-ring mounted directly to the end of the work roll. A general sketch for the data acquisition system is shown in Figure 5.

3.2. Ultrasonic pulsing and receiving instrumentation

To generate an ultrasonic pulse a voltage signal is used to excite the piezoelectric transducers and thus produce an ultrasonic wave. Returned waves reflected at contact interfaces are captured by the reverse of this process.

The voltage signal produced by the pulser typically takes the form of an inverted top hat. Signals of magnitude ~50 V are used in the following tests. The signal width defines its frequency which in-

turn affects the frequency content of the ultrasonic pulse produced. To get the best response the voltage signal frequency was matched to the centre frequency of the transducers.

The returned signal is amplified and then digitised at 100 MHz. The digitised signal is passed to a PC for processing. The signal is processed in real-time using bespoke software. Frequency spectra are taken using a fast Fourier transform (FFT).

The piezo transducers generate radio frequency (RF) electrical signals. The combination of high-pulsing voltage, short rise and fall times, high pulse repetition rate, low response voltage and the high rate of digitisation required make typical data acquisition equipment unsuitable. Therefore, specialised ultrasonic pulse generation and digitisation equipment is required. This took the form of a set of PCI cards which were mounted within an industrial PC chassis. The hardware is controlled and the data processed with custom software written in NI LabVIEW.

3.3. Rolling mill

Ultrasonic measurements are made during rolling experiments carried out on a pilot mill. This mill (see Figure 6 – a) is a 2-high-stand configuration where tensions, rolling speeds, forces and lubrication conditions representative of industrial applications are achievable.

Once the metal plug is pressed into the roll, the roll surface is grinded to avoid any geometrical discontinuity between the roll and the plug. The roll surface around the plug position after grinding is shown in Figure 6 – b and the plug position is barely visible. Consequently, perturbations due to the presence of the plug on the rolling condition are expected to be small.

However, during the tests, slight marks were left by the plug on the strip. They are due to the large contact pressure involved in these tests (the numerical model predicted maximal pressure values between 450 and 600 MPa for the different tests presented in this paper).

These small marks are acceptable for the testing conducted on the pilot mill but they prevent the present system to be used on an industrial mill on a daily basis since they would be detrimental to further metal processing such as stamping.

11

Ultrasonic roll bite measurements in cold rolling – roll stress and deformation

4. Ultrasonic measurements

The signals reflected back to the longitudinal sensor as a function of time (A-scan) are presented in Figure 7 for two sensors positions: outside and inside the roll bite. We can clearly see a shift in time between these two signals. As mentioned in section 3, this shift is due to roll deflection, acousto-elastic effect and phase shift. There is also a decrease in amplitude observed when the sensor is facing the roll bite. This is due to a part of the signal amplitude crossing the interface between the roll and the strip.

From the curves in Figure 7, it is possible to determine the change in ToF between two signals. The easiest method is the zero-crossing. It consists in measuring the time difference between two similar points of the two curves, for instance, the intersection between the signal after its maximum peak and the horizontal axis. Since this method is affected by phase shift, an approach which utilises the Hilbert envelope of the pulse is being used to calculate the ToF.

The Hilbert operator transforms a real signal, here the acoustic reflection, into a convolution with $1/(\pi t)$. The complex signal made of the real signal and the Hilbert transform as the imaginary part is called an analytic signal. By calculating the magnitude of this analytic signal, we obtain the envelope of the acoustic reflection (see Figure 8).

The change in ToF between two acoustic reflections is determined by measuring the time difference between two similar points of the corresponding Hilbert envelope. A common practice is to measure this difference at the maximum value of the envelope (see yMax in Figure 8). However, interferences occur with the acoustic reflection close to the roll bite entry and exit and the position of the maximum is affected.

To achieve more accurate results, a threshold - as calculated from a percentage of the maximum envelope value - is set and the point at which the envelope crosses this threshold is used to calculate the time of the pulse (see point p in Figure 8). The threshold is calculated as a percentage of the maximum as this removes the effect of any amplitude change in the reflected pulse. A low

12

Ultrasonic roll bite measurements in cold rolling – roll stress and deformation

percentage value is chosen to ensure the threshold is crossed at a time close to the start of the pulse, so that any interfering reflections occurring later in the time domain have a lesser effect.

The ToF variations obtained through this methodology with a threshold of 10%, 15% and 20% are presented in Figure 9. The reference signal chosen is an A-scan measured when the sensor is outside the roll bite (see Figure 8), at a horizontal distance of 55 mm ahead of the roll bite centre where the roll deflection is negligible. By comparison, the roll bite length L computed with the numerical model presented in the next section is 13.8 mm.

As expected, the ToF variation is negative which means the distance between the ultrasonic sensor and the roll surface decreases and the radial stress in the roll increases.

The magnitude of ToF variation becomes larger as the sensor reaches the roll bite where the maximum ToF absolute value is achieved. Then the ToF magnitude decreases as the sensor is moving away from the roll-strip interface.

The curves of ToF variation are smooth except in two zones close to the roll bite entry and exit, respectively named i_1 and i_2 in Figure 9. In these areas, there are distinct perturbations in the recorded ToF variation.

These perturbations arise from the fact that the roll bite is being measured with a finite size sensor. The whole face of the sensor emits sound waves that travel towards the contact. The waves hit the contact at slightly different times and bounce back interfering with each other. This effect is more pronounced at the entry and exit regions where part of the wave is being reflected from metal-air contact and part from metal-metal contact. This causes an interference fringe pattern (rather like overlapping ripples in a pond) and leads to the bumps in the ToF response. This interference effect has been observed in related work on measurements of rolling bearing contacts and is discussed at length by Howard (2016).

Ultrasonic roll bite measurements in cold rolling – roll stress and deformation

The extent of the roll bite length computed with the numerical model presented in the next section is added on top of the curves. This confirms that the area i_1 and i_2 are located close to the entry and the exit of the roll bite.

A curve showing the expected shape obtained if the interference fringes were not present is added in Figure 9. It is based on a manual drawing added on top of the three curves computed with different threshold values. The purpose of this is to show the reader an idea of the shape of the computed curve if the bumps presents in the zones denoted i_1 and i_2 were not present on the diagram.

Measurements carried out around the roll bite centre are not affected by these interferences. This area close to the roll bite centre is the most important since the largest roll deflection and radial stresses occur there.

There are two possible routes for reducing the effects of the interferences that limit this approach. Firstly, the more focussed the sound field the better (compared to the size of the roll-bite width). This could be achieved by using a smaller transducer and focusing through a lens. Commercial transducers that focus the wave using a concave lens can focus down to about 100 μm. This would significantly enhance the resolution, and remove fringe effects. However, focusing is normally done with the transducer immersed in a water bath; and conceiving of this arrangement in a metal rolling application is difficult. A second approach would be to accept that interference occurs and try to remove it by some numerical procedure. This would require the mapping out of the sound field and its reflection at the interface. Conventional ray tracing software would be suitable, but a model would have to be created for each rolling case.

It is also important to note that the vertical position of the threshold does not affect the results out of the two zones where interferences occur. It was decided to use a value of 10% to compute the results discussed in this paper. Indeed, this value reduces the amplitude of the bumps encountered in i_1 and i_2.

14

Ultrasonic roll bite measurements in cold rolling – roll stress and deformation

The change in ToF is converted in plug length variation and mean radial stress in the plug in section 6. There, experimental data are compared with numerical results for different rolling conditions encountered during the testing. The assumptions made in the numerical model are discussed in the next section.

5. Numerical Simulation

Cold rolling is a mechanical process which implies many complex mechanisms at different scale levels such as the stand elastic deformations, roll-flattening, elasto-plastic deformations of the strip, interactions between the asperities of the rolls and the strip, lubricant flow in the roll-bite, etc.

Several types of numerical methods, ranging from 1D to 3D, are available to model cold rolling depending on the process parameters and the required precision on the results. Montmitonnet (2006) gives a review of rolling numerical models. 3D models are usually employed to study flatness defects. On the other hand, when these defects can be neglected, cheaper 2D models can be used, particularly for very small thickness reductions. However, 1D models are sometimes sufficient and cheaper in terms of computational time. According to Montmitonnet (2006), in the case of flat products, "a 1D model is perfect for a ratio between the length of the roll bite and the strip thickness higher than 3". One of these 1D models has been developed by Marsault (1998) to account for the mixed lubrication regime in cold rolling. Stephany (2008) extended the capabilities of the model by including the effect of starvation, which is important when modelling rolling conditions lubricated with emulsions. Carretta et al. (2011) used this model to investigate rolling conditions encountered on an industrial rolling mill.

To validate the ultrasonic experimental measurements, numerical simulations were conducted with METAFOR (2016), an in-house dynamic implicit finite element (FE) code developed to model metal forming processes. For instance, Boman et al. (2006), and Boman and Ponthot (2012) used this software to model roll forming processes. Boman and Ponthot (2002) as well as Boman and Ponthot (2004) carried out cold rolling simulations in the hydrodynamic lubrication regime whereas Ponthot (2002) conducted superplastic forming simulations.

Ultrasonic roll bite measurements in cold rolling – roll stress and deformation

The Finite Element method is perfectly suited for the current application since strain and stress gradients can be computed on the roll and the strip. Numerical simulations were conducted in 2D assuming plane strain conditions. This assumption is valid in the present case since the width of the strip rolled during the testing is 100 mm and the strip thickness reduction is large. The 3D effects that might occur due to roll bending are therefore negligible.

5.1. Mesh and geometry

The model geometry is presented in Figure 10. Due to symmetry, only the upper roll and the half strip thickness are modelled.

An important feature of this rolling model is the use of the Arbitrary Lagrangian Eulerian (ALE) formulation for the strip. Unlike the classical Lagrangian formulation, where the material sticks to the mesh, the ALE method allows us to uncouple the motion of the material and the mesh. In the present case, this methodology is useful to define a refined mesh for the strip in a region close to the roll bite. Therefore, during the simulation material is constantly crossing the left and right boundaries of the strip domain, reducing the number of finite elements needed for strip discretisation. Boman and Ponthot (2002) as well as Boman and Ponthot (2004) have already successfully used the ALE formalism to model cold rolling conditions with the FE software METAFOR.

The mesh of the initial configuration is depicted in Figure 11. As shown in Figure 11 – c), the strip is spatially limited around a region where plastic deformations occur. The mesh is globally fixed in the main direction of the process even though the vertical node position is continuously adapted throughout the simulation.

A transfinite mesher is used on the strip and on the sector of the roll located close to the roll bite (see Figure 11 – b) – c)). The depth of the transfinite mesh on the roll is $d_0 = 34.77$ mm which corresponds to the distance between the ultrasonic sensors and the roll surface in the initial configuration. This regular part of the mesh is important to compute smooth displacement and stress fields in the area covered by the ultrasonic sensor during the testing.

Ultrasonic roll bite measurements in cold rolling – roll stress and deformation

The remaining part of the roll is meshed with an implementation of the unstructured quadrilateral mesh generation technique presented by Sarrate and Huerta (2000). Thanks to this mesher, the element size can be gradually increased as the distance from the roll bite increases (see Figure 11 – a)). The total number of elements for the roll and the strip is 4102.

The roll is Lagrangian which means the material of the roll sticks to the mesh. This feature is important to keep track of the boundaries of the area covered by the ultrasonic sensors during rolling. In this way, it is possible to compute the variation of the radial distance between the sensor position and the roll surface (plug length variation) to make a comparison with the experimental measurements.

In these simulations, four-node elements are used. Stresses are determined using a selective reduced integration method, the deviatoric part of the stress increment is computed at four Gauss points. The pressure increment is computed at the element centre, and then, assumed constant all over the element and transferred as such to the 4 Gauss points (SRIPR elements). As observed by Ponthot (1995) this allows us to avoid both volumetric locking as well as hourglass modes.

5.2. Material law

The plastic behaviour of the strip has been modelled thanks to the isotropic hardening law given in 1D by the following relation:

$$\sigma_y = (451 + 152\bar{\varepsilon})(1 - 0.3\exp(-9.13\bar{\varepsilon})) \quad [\text{MPa}] \tag{9}$$

The parameters have been identified on plane strain compression test results been performed internally by ArcelorMittal. The roll has an elastic behaviour and is attributed a Young's modulus of E = 210 GPa and a Poisson's ratio ν=0.3.

5.3. Contact and boundary conditions

The loading phase is divided into three stages (see Figure 12). Initially, the strip is rectangular. During the first step of the simulation, a vertical displacement is applied to the roll to indent the strip. Then, entry and exit strip tensions are applied gradually and the roll speed – applied on the inner

17

Ultrasonic roll bite measurements in cold rolling – roll stress and deformation

cylindrical axis- increases with a constant acceleration until the prescribed rolling velocity is achieved. Finally, during the third stage the velocity and the strip tensions are kept constant. The simulation goes on until steady state is achieved.

The contact algorithm is the penalty method. The normal contact force (F_N) computed with this method, on each slave node, is proportional to the normal gap (G_N), between the roll and strip surfaces, the normal penalty (C_N) and the area associated with each slave node A_{slave}. Wautelet and Ponthot (2014) computed the nodal area for 2D cases while Wautelet et al. (2016) presented the same methodology for 3D configurations.

$$\frac{F_N}{A_{slave}} = C_N G_N \tag{10}$$

$C_N = 10^5$ MPa/mm is used in the simulations discussed here.

In cold rolling, the motion of the strip is generated by the rotation of the two work rolls. Thus, friction is a key element in the process. In this model, friction is modelled with the well-known Coulomb's friction law. For each test conditions studied here, the friction coefficient (μ_C) is adjusted on the rolling load and forward slip values measured during the testing.

The time integration is performed using the implicit dynamic scheme developed by Chung-Hulbert (1993).

5.4. Plug length variation and mean radial stress

The finite element model gives a wide range of results such as stress profiles, plastic deformations, displacement and velocity fields, etc. In this study, displacement fields and radial stresses in the roll are processed to compute the plug length variation and the mean radial stress.

The plug length variation ($\delta(x) = d(x) - d_0$) is computed as the distance between two ranges of nodes initially located respectively on the roll surface and inside the roll, at distance $d_0 = 34.77$ mm from the surface (see Figure 3)

Ultrasonic roll bite measurements in cold rolling – roll stress and deformation

The mean radial stress is also computed from the finite element results. For each angular position, the radial stress field is integrated along r-direction between the sensor position and the roll surface and divided by the length along r. These results are fully discussed in the next section.

6. Comparison between experimental and numerical results

In this section, experimental measurements in terms of plug length variation and mean radial stress in the external roll layer are compared to numerical results.

Comparisons are made for three rolling conditions. The inlet and outlet strip tensions are respectively 38 MPa and 119 MPa. The roll radius is 195.5 mm, the rolling velocity is 100 m/min and the inlet strip thickness is 2.8 mm. Three strip elongation values are investigated: 20% - 30% - 40%. For each of these three test conditions, respectively denoted #1 - #2 - #3, the friction coefficient value of the rolling model is adjusted to match the rolling load and the forward slip measured experimentally.

6.1. Plug length variation

The plug length variation obtained experimentally for a strip elongation of 30% is presented in Figure 13. The experimental curve exhibits the same patterns as the curve of ToF variation discussed in section 4.

The corresponding FE results are compared to the experimental ones. The values for the position along the roll bite used in the modelling have been shifted to match the coordinate system used by the experimental data.

The main differences in the two curves occur close to the roll bite entry (between -6 and -1 mm) and exit (2 and 5 mm) where interferences in the recorded signals take place. Apart from these two zones, there is a good agreement between experimental and numerical curves. Before -5 mm and after 5 mm from the roll bite centre, experimental and numerical curves exhibit the same shape and are very close to each other. Moreover the values at the centre of the roll bite are practically identical: -37 μm for the experimental measurement and -38 μm for the FE results.

Ultrasonic roll bite measurements in cold rolling – roll stress and deformation

6.2. Radial roll stress

The evolution of the mean radial stress between the ultrasonic sensors and the roll surface while rolling is represented in Figure 14. The experimental curve is obtained from the plug length variation through equation 8. Therefore the radial stress curve has the exact same shape as the plug length variation curve discussed above.

The mean radial stress profile computed with the FE results has the same trend as the measurements (out of the zones affected by interferences).

At the roll bite centre, the experimental measurements give a value of -225 MPa while the numerical model provides -264 MPa. This represents a relative difference of 18% which is acceptable for the present purpose.

There is an offset between the two curves of around 35 MPa. This is most certainly due to the 1D stress state assumption made to determine σ_r from experimental measurements. However, this simple formula provides a good estimation of the mean radial stress close to the roll surface.

With such experimental procedure, by performing experiments where the ultrasonic sensors are closer to the roll surface, it would be possible to measure the pressure profile in the roll bite which is an important feature in the field of cold rolling. However, moving the sensor closer to the roll subjects it to greater stress and possible damage. The shorter plug also has the potential to upset the distribution of stress around the roll bite region.

6.3. Effect of strip elongation on the plug length and roll stress

The effect of strip elongation on plug length variation is presented in Figure 15. As expected, a larger strip elongation leads to a larger rolling load and therefore a larger plug length variation. The trend is similar for experimental and numerical results. Moreover, there is very good agreement between these two types of data. The difference is 1 μm for each of these three cases.

The trend observed in Figure 16 for the maximum absolute value of the roll radial stress in the roll bite is similar: the larger the strip elongation the larger the radial stress. Once again, both numerical

Ultrasonic roll bite measurements in cold rolling – roll stress and deformation

and experimental results exhibit the same trends but the difference is more important in that case. The maximum relative difference observed here, 18%, is achieved for a strip elongation of 30%.

7. Conclusion

Ultrasonic sensors were used on a pilot mill to carry out measurements in the contact zone between the upper roll and the strip during cold rolling of thin metal sheet. By computing the change in Time of Flight of the reflected pulse from the roll surface, it was possible to determine the deflection of the external layer of the roll as well as the mean radial stress in that area.

Interferences occurred during the testing close to the entry and the exit of the contact zone between the roll and the strip. They induced some noise which makes the measurements less reliable in these two areas. Everywhere else, before the contact, after the contact and within the roll bite, experimental measurements were smooth. It is an important feature since this is the area where the roll deformation and radial stresses are the largest.

Experimental measurements were compared to numerical results computed with a finite element model of cold rolling implemented in a non-linear Finite Element code. This comparison was conducted for three different strip elongations of 20%, 30% and 40%. For these different tests conditions, numerical results and experimental data exhibited the same trends and were very close to each other both in terms of roll deformation and mean radial stresses. Thus, these two techniques validate each other and the reliability of the measurement system is proven.

The experimental methodology presented in this paper proved to be suitable for in situ and real-time measurements in the roll bite of a pilot mill. This is very useful to get a better understanding of the phenomena involved in the process when conducting some testing on the pilot mill.

The weakness of the present system holds in the use of a metal plug to fit the ultrasonic sensor in the roll. Indeed, even though precautions were taken in order to reduce as much as possible the influence of the plug – such as regrinding the roll surface after pressing the plug into the roll – slight

Ultrasonic roll bite measurements in cold rolling – roll stress and deformation

marks were observed on the strip after rolling. This is due to the large contact pressure involved in these tests (the numerical model predicted maximal pressure values between 450 and 600 MPa for the different tests presented in this paper). Therefore, the current system cannot be used as it is on an industrial rolling mill and the present work is an intermediate step proving the concept validity.

To be used on an industrial mill on a daily basis, a method that has sensors on the outside of the roll has to be developed. In such case, two sensors (an emitter and a receiver) would be located on the two barrel end surfaces of the roll. The emitter would send an ultrasonic wave towards the roll-bite which would reflect the acoustic wave towards the receiver. Once such system is available, several measurements conducted at the same time along the roll axis with different sensors would give pieces of information such as roll flattening and differential strip elongation. Therefore, thickness homogeneity and differential elongation along strip width could be evaluated in real time allowing mill operators to react efficiently by changing the cooling configuration of the roll, lubricant conditions, etc.

References

Anderson, W., Jarzynski, J. and Salant, R.F., 2001, A Condition Monitor for Liquid Lubricated Mechanical Seals, Tribology Transactions, 4, 801-806.

Arakawa, T. (1983), A study on the transmission and reflection of an ultrasonic beam at machined surfaces pressed against each other, Materials Evaluation, 41, 714-719.

Baik, J-M and Thompson, R.B., 1984, Ultrasonic scattering from imperfect interfaces: a quasi-static model, Journal of Non-destructive Evaluation, 4, 177-196.

Ultrasonic roll bite measurements in cold rolling – roll stress and deformation

Baltazar, A., Rokhlin, S., and Pecorari, C., 2002, On the Relationship between Ultrasonic and Micromechanical Proerties of Contacting Rough Surfaces, Journal of the Mechanics and Physics of Solids, 50,1397-1416.

Boman, R., Ponthot, J.-P., 2002. Numerical simulation of lubricated contact in rolling processes. Journal of Material Processing Technology. 125–126,407–413.

Boman, R., Ponthot, J.-P., 2004. Finite element simulation of lubricated contact in rolling using Arbitrary Lagrangian Eulerian formulation. Computer Methods in Applied Mechanics and Engineering. 193(39–41),4323–4353.

Boman, R., Papeleux, L., Bui, Q.-V., Ponthot J.-P., 2006. Application of the Arbitrary Lagrangian Eulerian formulation to the numerical simulation of cold roll forming process. Journal of Material Processing Technology. 177, 621–625.

Boman, R., and Ponthot, J.-P., 2012. Efficient ALE mesh management for 3D quasi-Eulerian problems. International Journal for Numerical Methods in Engineering. 92(10), 857–890.

Carretta, Y., Boman, R., Stephany, A., Legrand, N., Laugier, M. and Ponthot, J.-P., 2011. MetaLub - A slab method software for the numerical simulation of mixed lubrication regime in cold strip rolling. Proceedings of the Institution of Mechanical Engineers, Part J: Journal of Engineering Tribology. 225(9), 894-904.

Chen, W., Mills, R., Dwyer-Joyce, R.S., 2015. Direct load monitoring of rolling bearing contacts using ultrasonic time of flight. Proceedings of the Royal Society of London A. 471: 20150103.

Chung, J., Hulbert, J.M., 1993. A time integration algorithms for structural dynamics with improved numerical dissipations: the generalized-a method. Journal of Applied Mechanics. 60, 371–375.

Drinkwater, B.W., Dwyer-Joyce, R.S., Cawley, P., 1996. A Study of the Interaction between Ultrasound and a Partially Contacting Solid-Solid Interface. Proceedings of the Royal Society of London A: Mathematical, Physical and Engineering Sciences. 452, 2613-2628.

Dwyer-Joyce, R.S., Drinkwater, B.W. and Quinn, A.M., 2000. The Use of Ultrasound in the Investigation of Rough Surface Interfaces. ASME Journal of Tribology, 123(1), 8-16.

Dwyer-Joyce, R.S., Drinkwater, B.W., and Donohoe C.J., 2002. The measurement of lubricant–film thickness using ultrasound, Proceedings of the Royal Society A. 459, 957-976.

Egle, D.M., Bray, D.E., 1976. Measurement of acoustoelastic and third-order elastic constants for rail steel. The Journal of the Acoustical Society of America. 60 (3), 741-744.

Howard, T.P., (2016), 'Development of a Novel Bearing Concept for Improved Wind Turbine Gearbox Reliability', University of Sheffield PhD Thesis, Sheffield, UK.

Hunter, A., Dwyer-Joyce, R. S., Harper, P., 2012. Calibration and validation of ultrasonic reflection methods for thin-film measurement in tribology. Measurement Science and Technology, 23 (10).

Kendall, K. and Tabor, D., 1971, An ultrasonic study of the area of contact between stationary and sliding surfaces, Proceedings of the Royal Society A. 323, 321-340.

Kräutkramer, J. and Kräutkramer, H., 1975. Ultrasonic testing of materials. Springer-Verlag, New York.

Krolikowski, J. and Szczepek, J., 1991, Prediction of contact parameters using ultrasonic method, Wear, 148, 181-195.

Ultrasonic roll bite measurements in cold rolling – roll stress and deformation

Legrand, N., Patrault, D., Labbe, N., Gade, D., Piesak, D., Jonsson, N.G., Nilsson, A., Horsky, J., Luks, T., Montmitonnet, P., Canivenc, R., Dwyer-Joyce, R.S., Hunter, A.K., Maurin, L., 2014. Advanced RollGap Sensors for enhanced hot and cold rolling processes, European RFCS project RFS-CT-2009-00008.

Marsault, N. 1998. Modélisation du Régime de Lubrification Mixte en Laminage à Froid. PhD dissertation (in French), Ecole Nationale Supérieure des Mines de Paris.

METAFOR: A large strain finite element software. University of Liège (LTAS-MN2L), 2016, http://metafor.ltas.ulg.ac.be/.

Mills, R., Vail, J., Dwyer-Joyce, R.S., 2015, Ultrasound for the non-invasive measurement of IC engine piston ring oil films, Proceedings of the Institution of Mechanical Engineers, Part J: Journal of Engineering Tribology, 229(2):207-215.

Montmitonnet, P., 2006. Hot and cold strip rolling processes. Computer methods in applied mechanics and engineering, 195, 6604-6625.

Nagy, P.B., 1992, Ultrasonic classification of imperfect interfaces, Journal of Non-destructive Evaluation, 11 (3/4), 127-139.

Ponthot, J.-P., 2002. Unified stress update algorithms for the numerical simulation of large deformation elasto-plastic and elasto-viscoplastic processes. International Journal of Plasticity, 18, 91–126.

Ponthot, J.-P., 1995. Traitement unifié de la Mécanique des Milieux Continus solides en grandes transformations par la méthode des éléments finis, Ph.D. Thesis (in French), University of Liège, Belgium.

Reddyhoff, T., Kasolang, S., Dwyer-Joyce, R. S., Drinkwater, B. W., 2005. The phase shift of an ultrasonic pulse at an oil layer and determination of film thickness. Proceedings of the Institution of Mechanical Engineers, Part J: Journal of Engineering Tribology. 219 (6), 387-400.

Sarrate, J., Huerta, A., 2000. Efficient unstructured quadrilateral mesh generation. International Journal of Numerical Methods in Engineering. 49,1327–1350.

Smith, O and Sutton, M, 2011, Fuel economy in heavy duty diesel engines. Part 1: measurement of oil film thickness on an operating engine , Proceedings of the Institution of Mechanical Engineers, Part J: Journal of Engineering Tribology 225, 313-324.

Stephany, A., 2008. Contribution à l'étude numérique de la lubrification en régime mixte en laminage à froid. PhD dissertation (in French), University of Liège.

Takeuchi, A., 2011, Investigation on lubrication condition of piston pin in real engine block with ultrasonic technique, Lubrication Science, 23, 331–346

Wautelet, G., Ponthot, J.-P., 2014. The influence of equivalent contact area computation in extended node to surface contact elements, Key Engineering Materials. 618, 1-22.

Wautelet, G., Papeleux, L., Ponthot, J.-P.,2016. The Influence of Equivalent Contact Area Computation in 3D Extended Node to Surface Contact Elements. Key Engineering Materials. 681, 19-46.

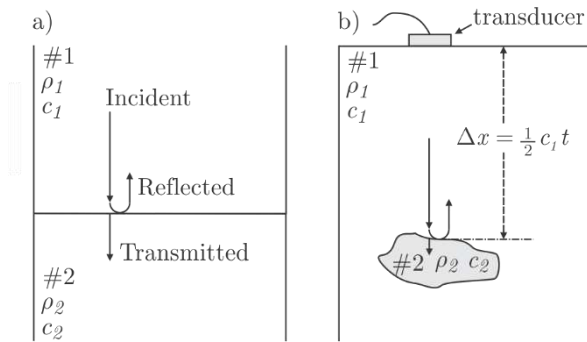Ultrasonic roll bite measurements in cold rolling – roll stress and deformation

Figure 1. a) Schematic view of an ultrasonic beam reaching the interface between two different media. A part of the incident wave is transmitted while the rest is reflected. b) Working principle of the ToF method used to detect flaws within material.
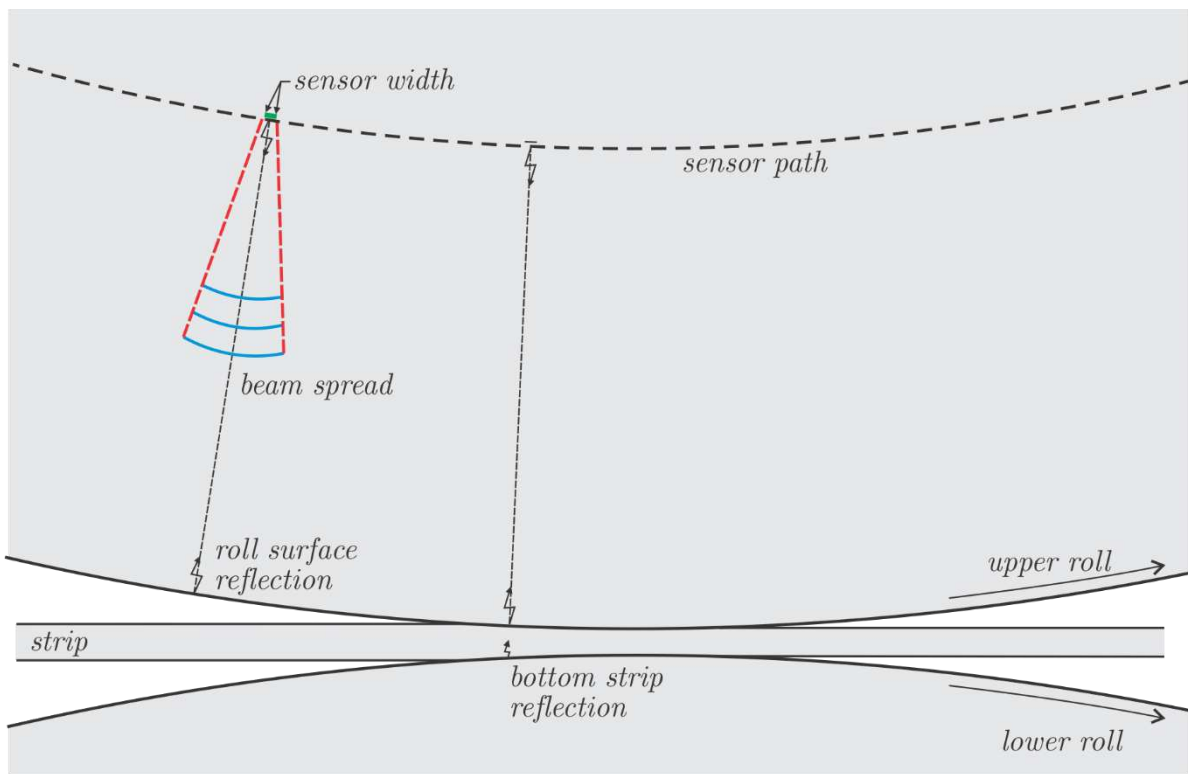

Figure 2. Ultrasonic reflections in cold rolling depending on the sensor position along its path. The initial distance d_0 (unloaded case) between the sensor and the roll surface is 34.77 mm. Except for the beam spread, the proportions are accurate for a 2.8 mm strip thickness undergoing a reduction of 40%.

25

Ultrasonic roll bite measurements in cold rolling – roll stress and deformation
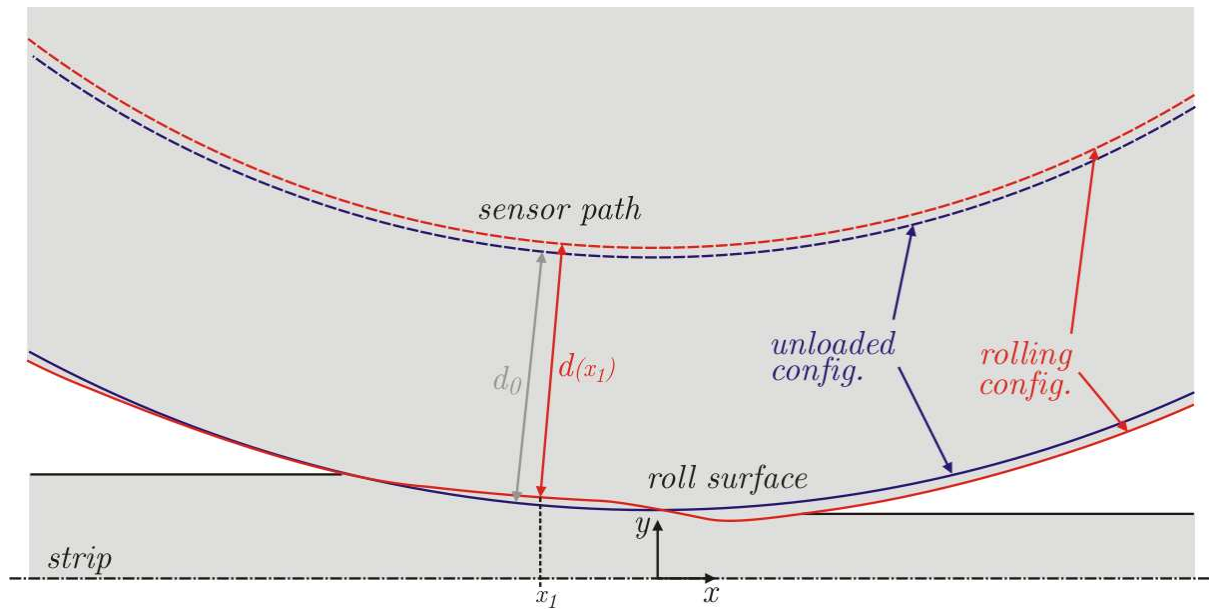
Figure 3. Comparison of the radial distance d*(x)*, between the sensor position and the roll surface (plug length) when rolling a metal strip, to the initial plug length d_0 when the roll is not subjected to any load. The plug length variation (δ) is the difference between these two configurations (δ(x) = d(x) – d_0).
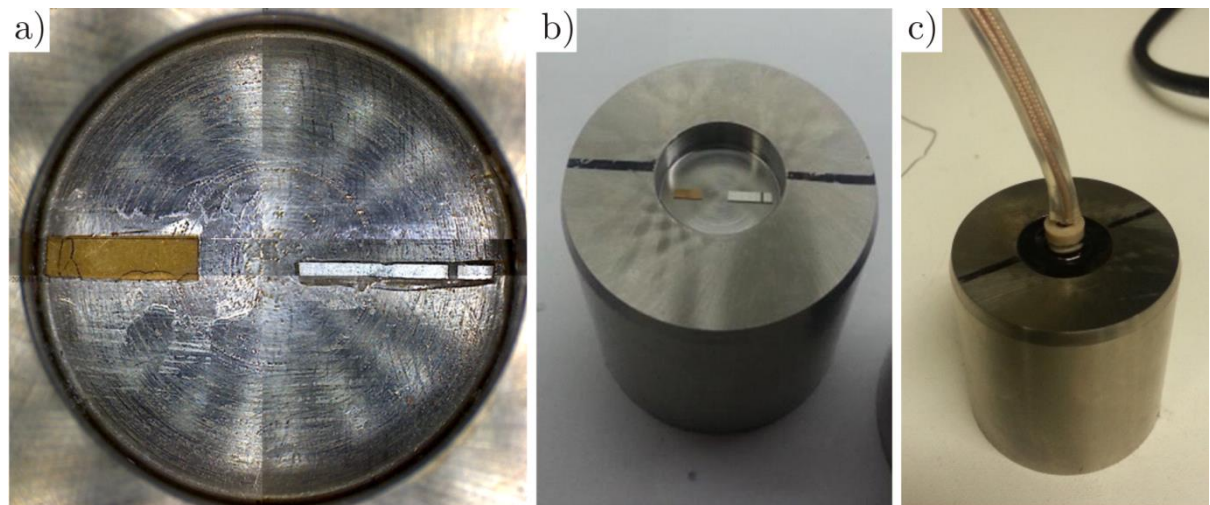
Figure 4. Metal plug, used in cold rolling testing, at various stages of instrumentation. a) Shear (left) and Longitudinal (right) sensors bonded to the top of the metallic part. b) Global view before sensor connection to the wires and epoxy covering. c) State of the plug before roll fitting.

Ultrasonic roll bite measurements in cold rolling – roll stress and deformation
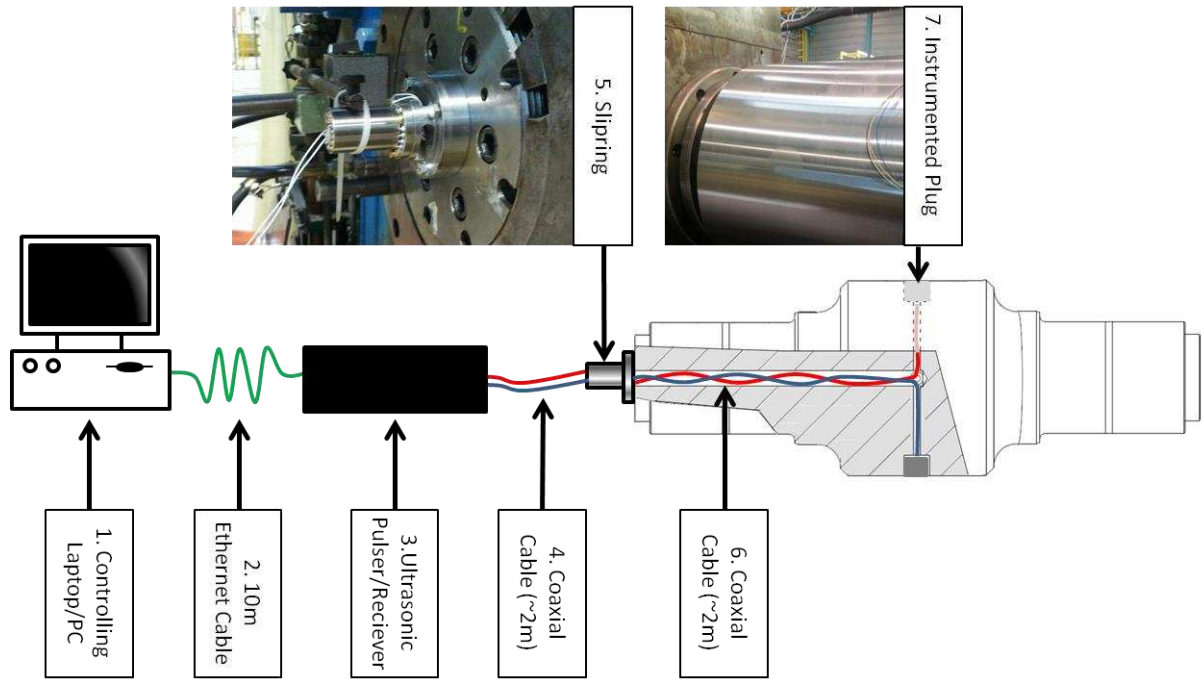
Figure 5. Ultrasonic data acquisition system overview. An ultrasonic pulser/receiver controlled by a computer is used to send and receive signals to and from ultrasonic sensors through coaxial cables connected to an instrumented plug.

Figure 6. a) ArcelorMittal pilot mill where ultrasonic sensors were tested. b) Roll surface, around the plug containing the ultrasonic sensors, after grinding. The geometrical discontinuity is reduced and the plug position is barely visible.

Ultrasonic roll bite measurements in cold rolling – roll stress and deformation
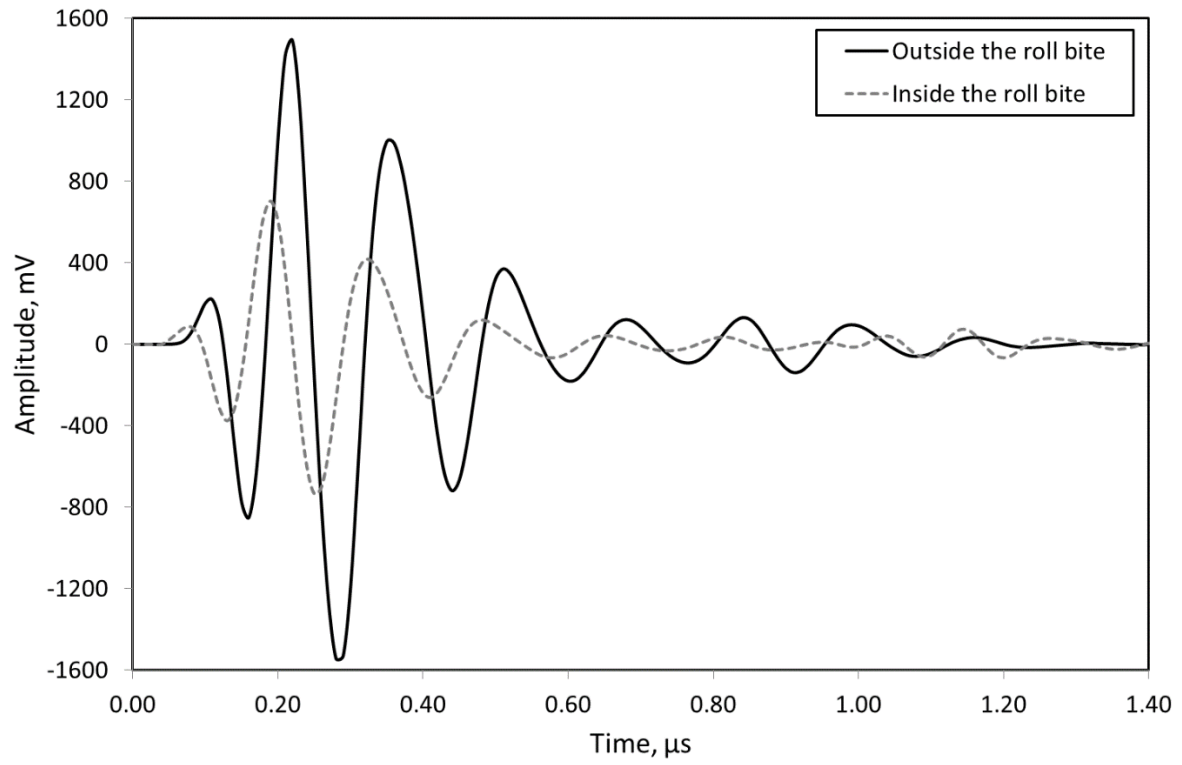
Figure 7. Reflections, from the roll surface outside and inside the roll bite, captured by the ultrasonic longitudinal sensor. The reflection from outside the roll bite (55 mm away from the roll bite entry) is taken as a reference for the computation of the ToF variation when rolling.

Ultrasonic roll bite measurements in cold rolling – roll stress and deformation
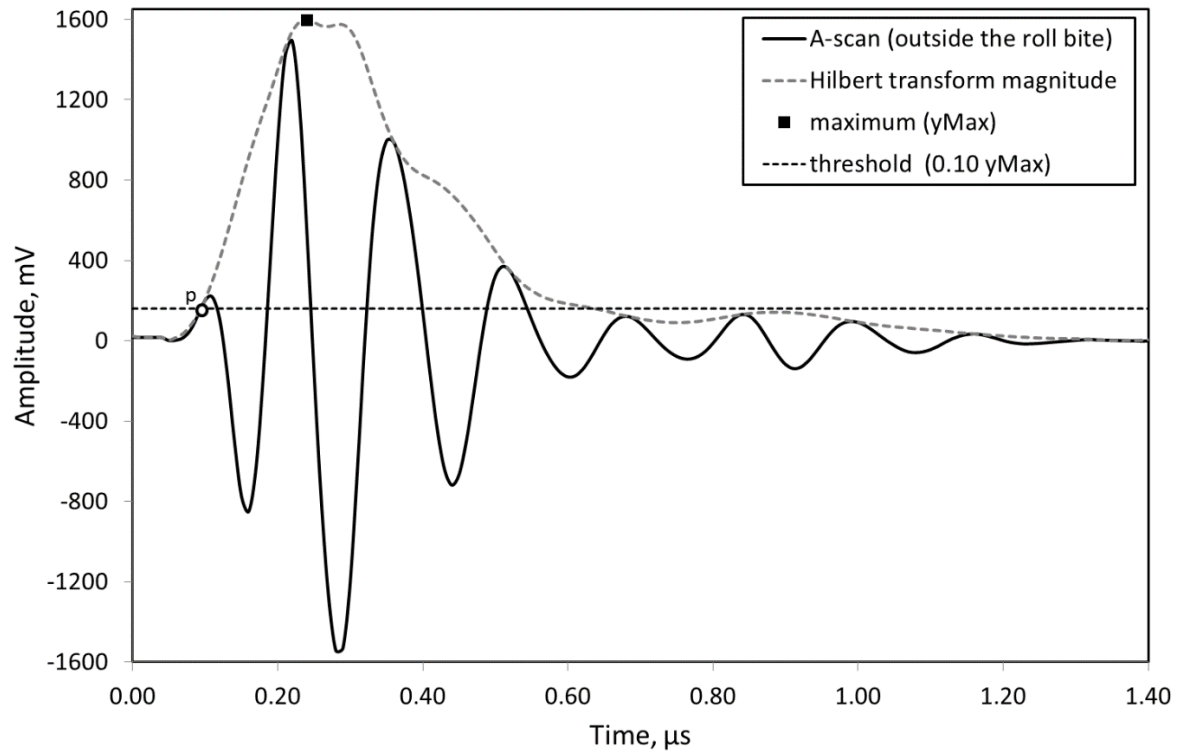
Figure 8. Hilbert envelope of the A-scan measured outside the roll bite and used as a reference for the computation of the ToF variation. The motion of point *p* – computed as the intersection between the Hilbert envelope and a horizontal line having an ordinate corresponding to 10% of the maximum value of the Hilbert envelope – is used to compute the ToF variation as the roll is rotating.

Ultrasonic roll bite measurements in cold rolling – roll stress and deformation
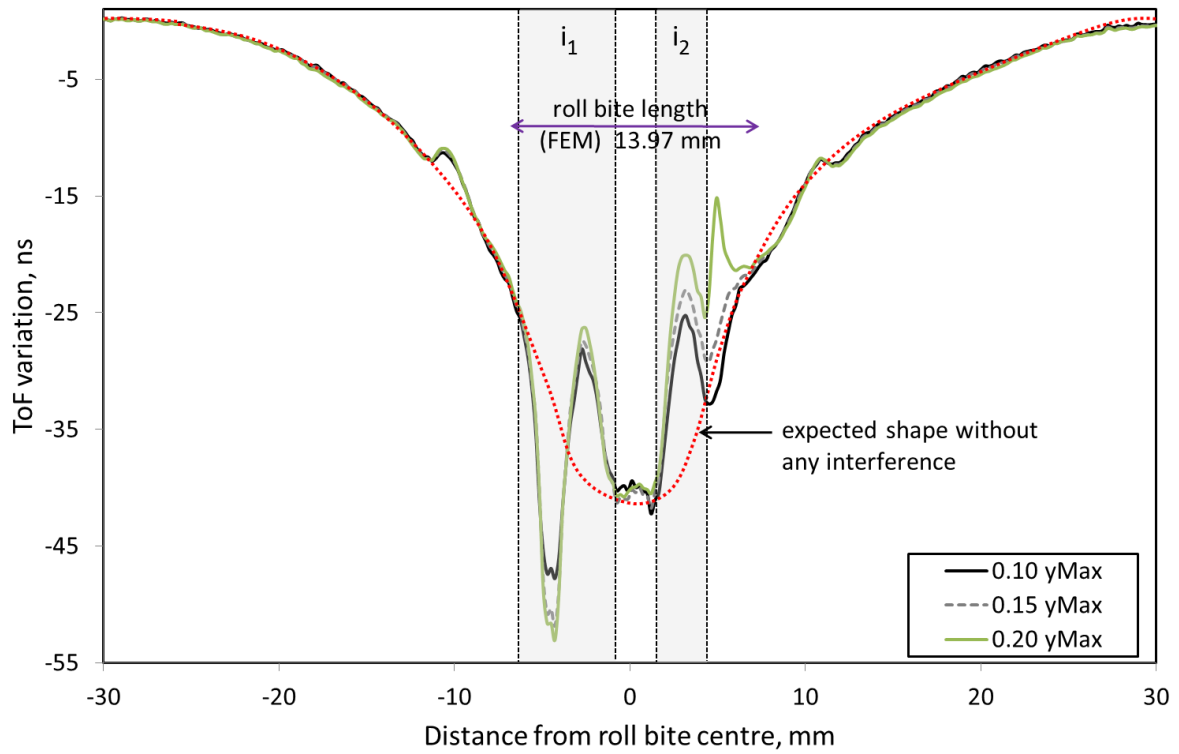
Figure 9. Time of flight variation of the acoustic reflection from the roll surface measured as the roll is rotating when rolling a metal strip with a strip elongation of 30%.
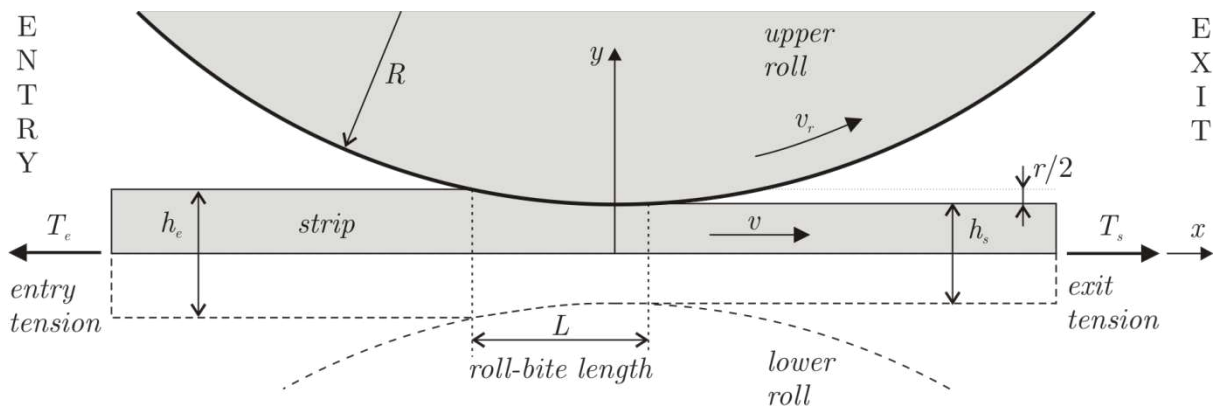
Figure 10. Finite element model geometry.

Ultrasonic roll bite measurements in cold rolling – roll stress and deformation
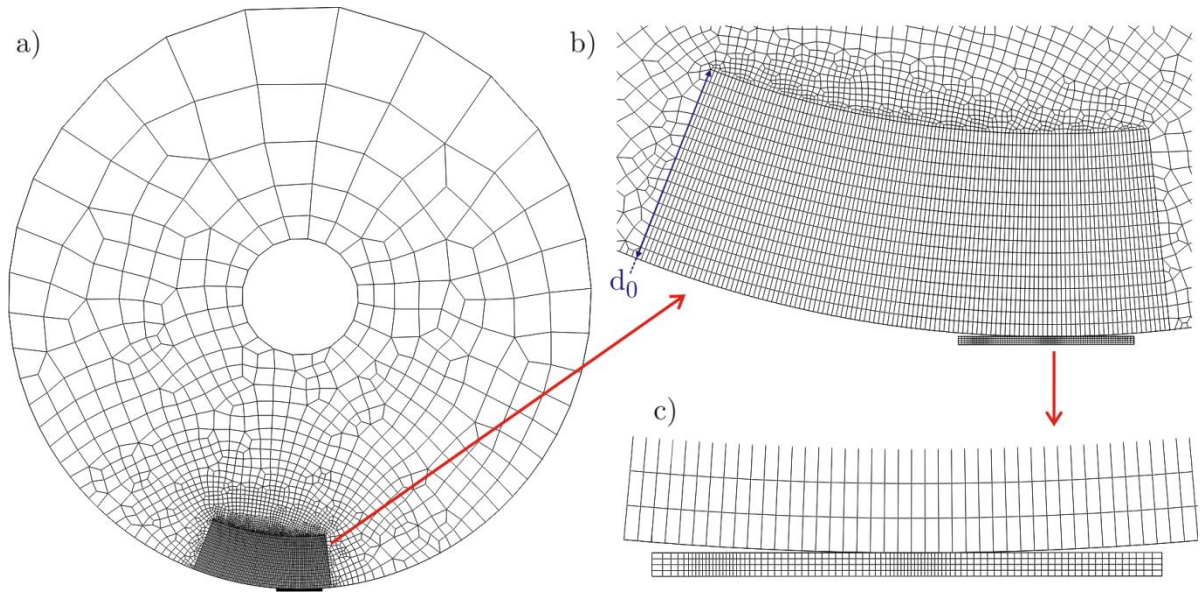

Figure 11. Finite element mesh in the initial configuration a) full roll b) roll section of interest and c) roll-strip interface.
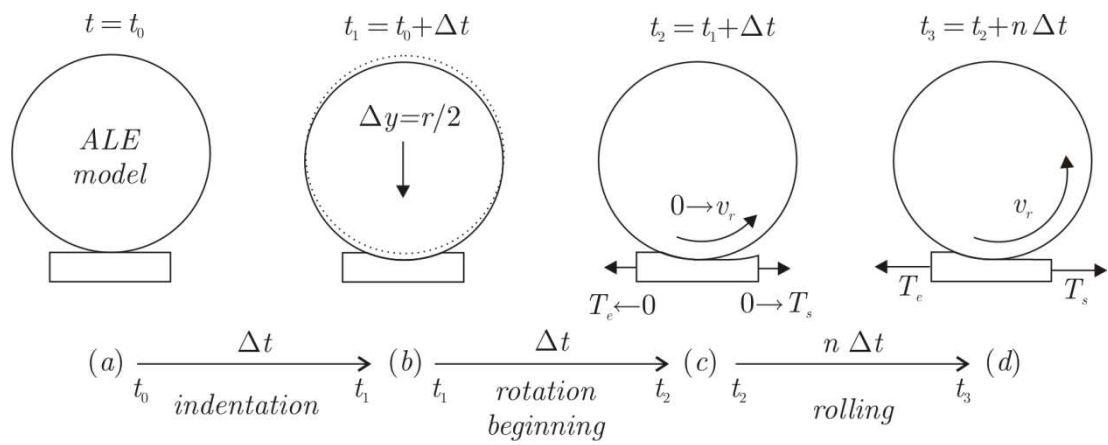

Figure 12. Different stages involved in the finite element simulation of cold rolling.

31

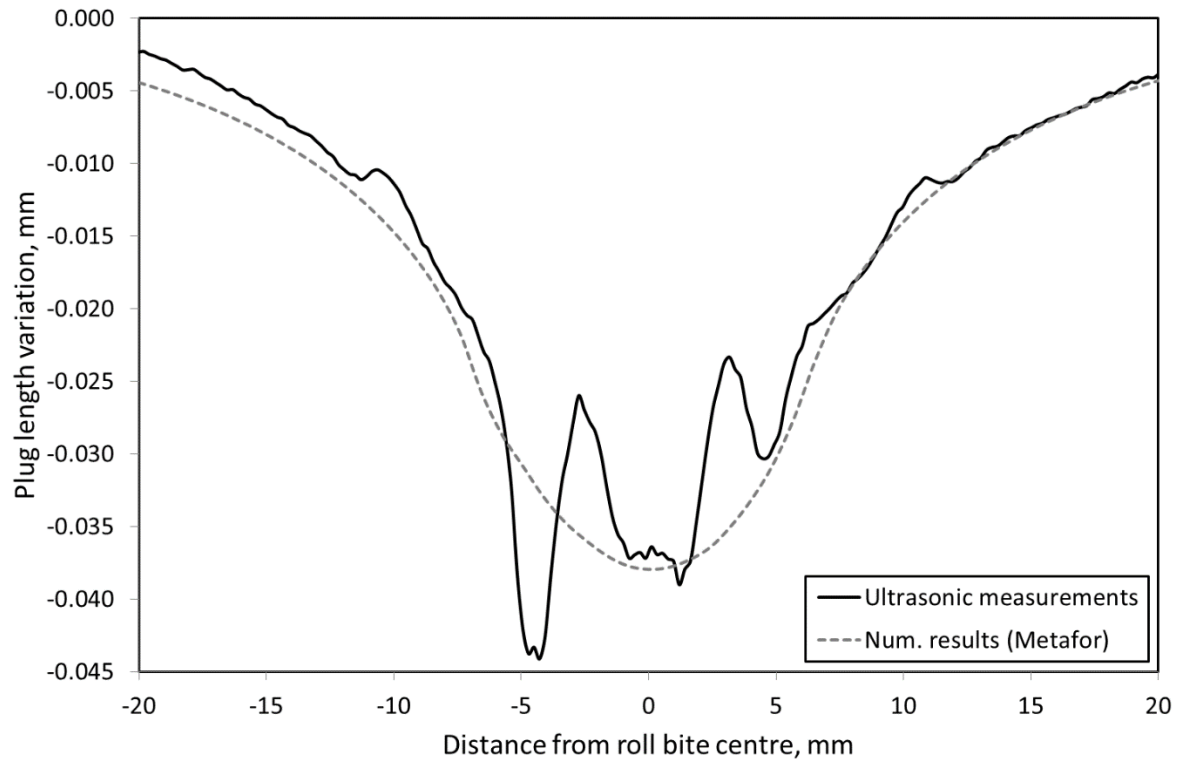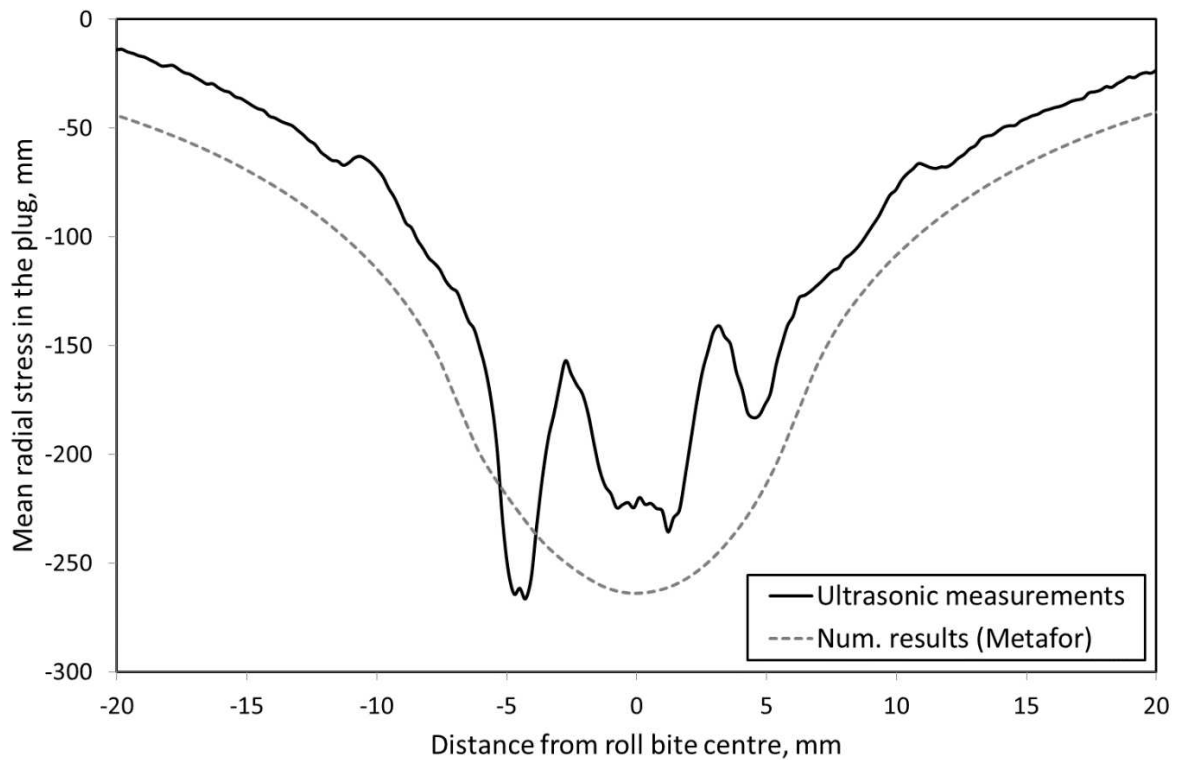Ultrasonic roll bite measurements in cold rolling – roll stress and deformation

Figure 13. Comparison of the plug length variation measured during test condition #2 (30% strip elongation) to the numerical results obtained with the FE model.

Ultrasonic roll bite measurements in cold rolling – roll stress and deformation

Figure 14 Comparison of the mean radial stress variation measured during test condition #2 (30% strip elongation) to the numerical results obtained with the FE model.
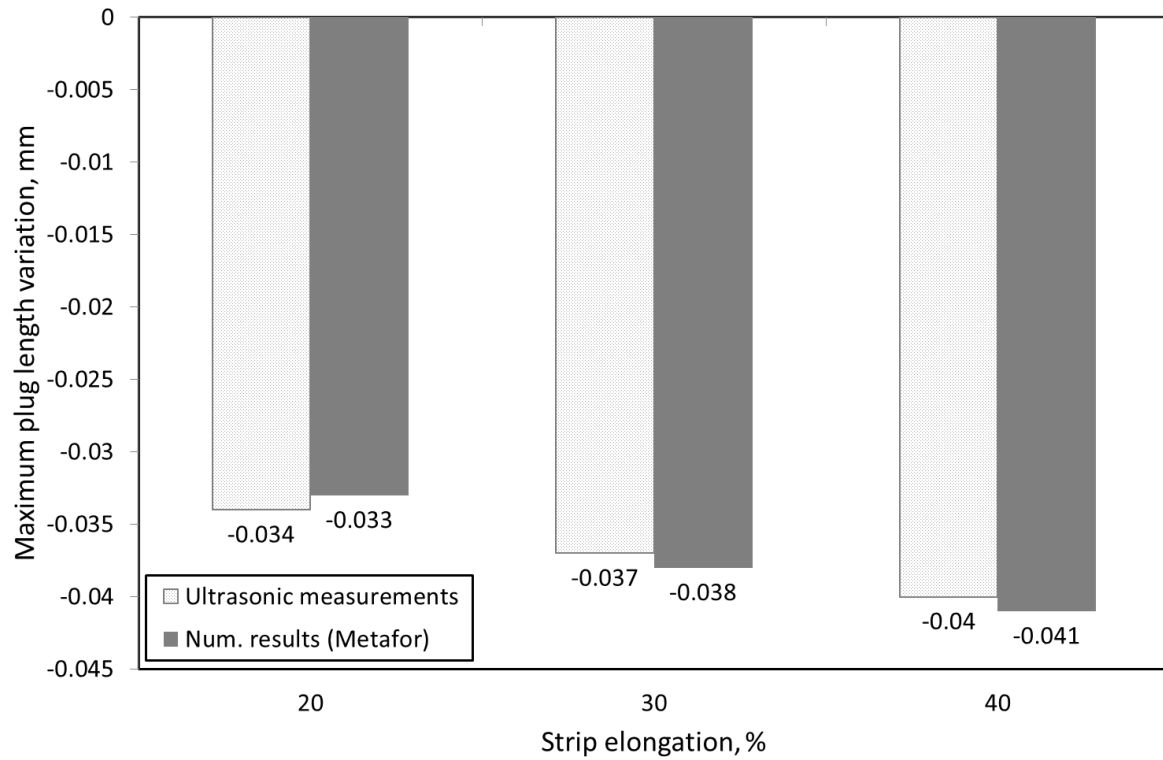

Figure 15. Maximum plug length variation for different strip elongation. Comparison of the ultrasonic measurements to finite element results.

33

Ultrasonic roll bite measurements in cold rolling – roll stress and deformation
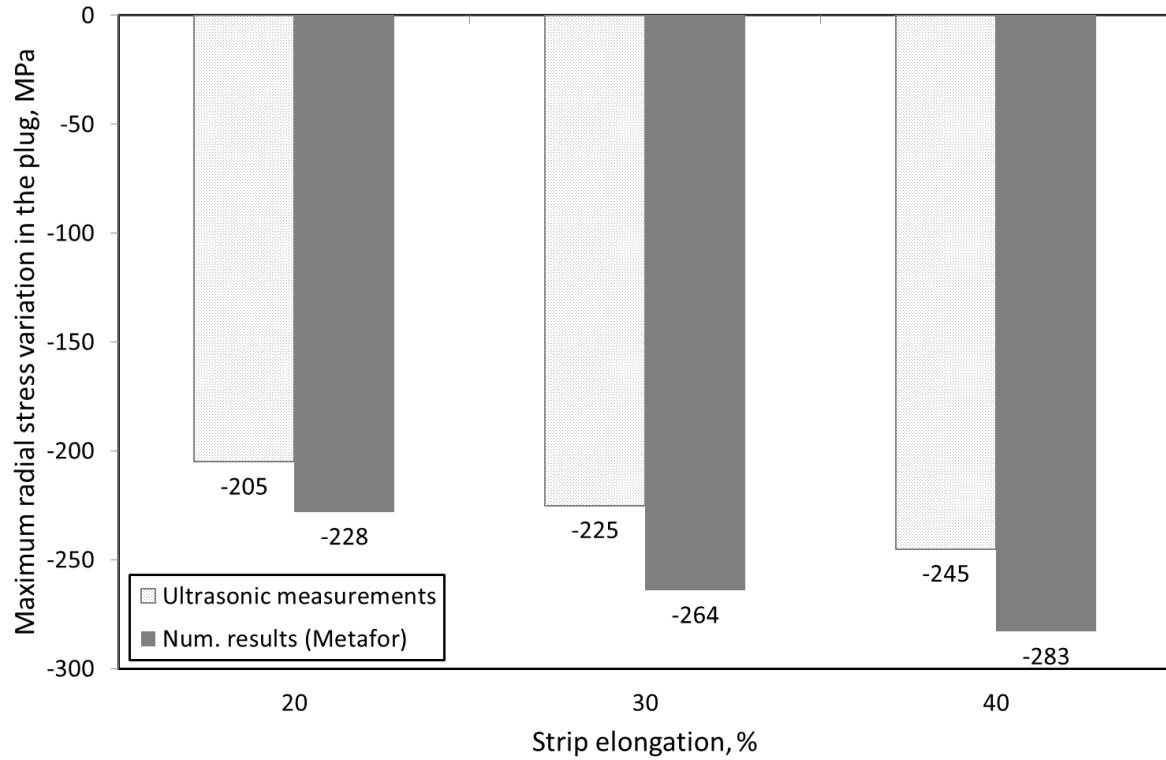

Figure 16. Maximum radial stress variation in the plug for different strip elongation. Comparison of the ultrasonic measurements to finite element results.

	C	Si	Cr	Mn
EN31	1.0%	0.20%	1.40%	0.50%

Table 1. Numerical values of the parameters involved in the computation of the plug length variation and the average radial stress in the plug based on the measurement of the change in ToF.

E [MPa]	d_0 [mm]	$(c_{rr})_0$ [mm/s]	α_{rr}
210 000	34.77	6000×10^3	-2.24

Table 2. Numerical values of the parameters involved in the computation of the plug length variation and the average radial stress in the plug based on the measurement of the change in ToF.